OPEN ACCESS Freely available online

PLOS ONE

A 5000-Fold Increase in the Specificity of a Bacterial Phosphotriesterase for Malathion through Combinatorial Active Site Mutagenesis

Tatheer Naqvi[1,2], Andrew C. Warden[2], Nigel French[2], Elena Sugrue[3], Paul D. Carr[3], Colin J. Jackson[3], Colin Scott[2]*

1 Department of Environmental Sciences, COMSATS Institute of Information Technology, Abbottabad, Pakistan, **2** Ecosystem Sciences, Commonwealth Scientific and Industrial Research Organisation, Canberra, Australian Capital Territory, Australia, **3** Research School of Chemistry, Australian National University, Canberra, Australian Capital Territory, Australia

Abstract

Phosphotriesterases (PTEs) have been isolated from a range of bacterial species, including *Agrobcaterium radiobacter* (PTE_{Ar}), and are efficient enzymes with broad substrate ranges. The turnover rate of PTE_{Ar} for the common organophosphorous insecticide malathion is lower than expected based on its physical properties; principally the pk_a of its leaving group. In this study, we rationalise the turnover rate of PTE_{Ar} for malathion using computational docking of the substrate into a high resolution crystal structure of the enzyme, suggesting that malathion is too large for the PTE_{Ar} binding pocket. Protein engineering through combinatorial active site saturation testing (CASTing) was then used to increase the rate of malathion turnover. Variants from a CASTing library in which Ser308 and Tyr309 were mutated yielded variants with increased activity towards malathion. The most active PTE_{Ar} variant carried Ser308Leu and Tyr309Ala substitutions, which resulted in a *ca.* 5000-fold increase in k_{cat}/K_M for malathion. X-ray crystal structures for the PTE_{Ar} Ser308Leu\Tyr309Ala variant demonstrate that the access to the binding pocket was enhanced by the replacement of the bulky Tyr309 residue with the smaller alanine residue.

Citation: Naqvi T, Warden AC, French N, Sugrue E, Carr PD, et al. (2014) A 5000-Fold Increase in the Specificity of a Bacterial Phosphotriesterase for Malathion through Combinatorial Active Site Mutagenesis. PLoS ONE 9(4): e94177. doi:10.1371/journal.pone.0094177

Editor: Renwick Dobson, University of Canterbury, New Zealand

Received January 28, 2014; **Accepted** March 12, 2014; **Published** April 10, 2014

Funding: TN was supported by an Australian Department of Industry Endeavour Fellowship. The funders had no role in study design, data collection and analysis, decision to publish, or preparation of the manuscript.

Competing Interests: The authors have declared that no competing interests exist.

* E-mail: colin.scott@csiro.au

Introduction

The World Health Organization has estimated that there are > 3,000,000 cases of pesticide poisonings annually, which result in approximately 200,000 deaths. Many of these cases are due to accidental or deliberate intoxication with neurotoxic organophosphate pesticides (OPs) [1].

OPs are potent cholinesterase inhibitors used extensively for the control of a variety of invertebrate pest species, but which also effect acute intoxication in humans [2]. The OPs share a phosphotriester structure, which is closely related to chemical warfare agents, such as VX and Sarin (Fig. 1). Enzymes that hydrolyse, and consequently detoxify, these phosphotriesters have been isolated from diverse origins [3,4]. The best described of these enzymes are the bacterial phosphotriesterases (PTEs).

PTEs have been isolated from a range of bacterial species, including *Pseudomonas diminuta* (PTE_{Pd}) and *Agrobacterium radiobacter* (PTE_{Ar}) [5,6]. They are binuclear metalloenzymes [7], highly efficient catalysts and display broad substrate specificities that include most phosphotriesters [5,6,8,9]. PTEs have therefore been investigated for applications in environmental monitoring, pesticide decontamination, nerve agent detoxification and in clinical applications [9–15].

The S_N2 mechanism of PTE, using a metal-activated water as the nucleophile, is well documented [16–18]. This mechanism results in a biphasic dependence of the rate of hydrolysis upon the pK_a of the leaving group of the substrate (Fig. 2). For OPs with leaving groups that have pK_a values of ~8.0 or lower the k_{cat}/K_M for the reaction is near the diffusion limit, while at pK_a values of greater than ~8.0 there is a linear relationship between pK_a and log (k_{cat}/K_M). Outliers to this trend have been documented, with their lower than expected turnover rates typically resulting from physical barriers to correct substrate binding, such as steric hindrance or non-productive binding [8,19,20].

The active site and substrate-binding pocket of the PTEs are also well defined, with an iron-zinc binuclear metal center co-ordinated by four histidine residues (His55, His57, His201 and His230) and aspartate (Asp301) and an unusual carbamylated lysine (Lys196), which bridges the center by co-coordinating both metals [7] (numbering for PTE_{Ar}). The substrate-binding pocket is comprised of a number of largely hydrophobic residues: Gly60, Ser61, Ile106, Trp131, Phe132, Arg254, Tyr257, Leu271, Leu303, Phe306, Ser308 and Phe309 in PTE_{Ar} [6,17–20]. The large, hydrophobic substrate-binding pocket can accommodate the majority of anthropogenic phosphotriesters [3,10,19], including insecticides and nerve agents, and is responsible for the broad substrate range of the enzyme.

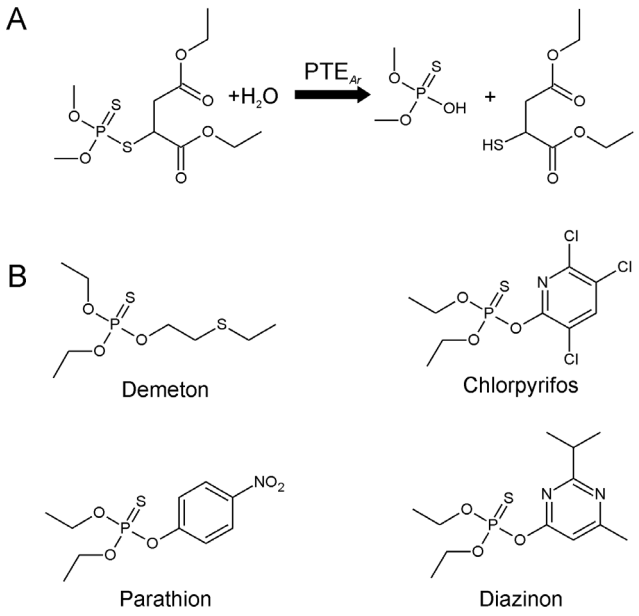

Figure 1. Hydrolytic activity of PTE$_{Ar}$. A) Schematic showing the PTE$_{Ar}$-mediated hydrolysis of malathion. B) Structure of the OP insecticides demeton, chlorpyrifos, parathion and diazinon.
doi:10.1371/journal.pone.0094177.g001

The efficiency of PTE against many such substrates, including chlorpyrifos, demeton-S, chlorfenvinphos, diisopropyl fluorophsphate and others, has been improved by directed (laboratory) evolution, rational design and incorporation of unnatural amino acids [18,20–24]. However, there have been no reports of substantial improvements in the turnover rate of PTEs towards malathion, the most widely used OP insecticide in the US [25] with significant applications in the control of West Nile virus and fruit fly infestation [26,27].

Herein we have used Combinatorial Active-Site Saturation Testing (CASTing) [28] to improve the efficiency of malathion turnover by reducing the rate limitation caused by steric hindrance of substrate binding.

Methods and Materials

Chemicals and reagents

All chemicals and reagents were obtained from Sigma-Aldrich. Malathion and its metabolites were of analytical grade and >99% pure. Synthetic oligonucleotides were obtained from GeneWorks (Australia). Restriction enzymes were obtained from New England Biolabs (Australia).

Bacterial growth

E. coli Bl21 (λDE3) was used for screening and production of variant enzymes and was cultured in LB, on LB supplemented with 1.5% w/v agar (LBA) or in Terrific Broth [29]. The media were supplemented with 100 μg.mL^{-1} ampicillin as required.

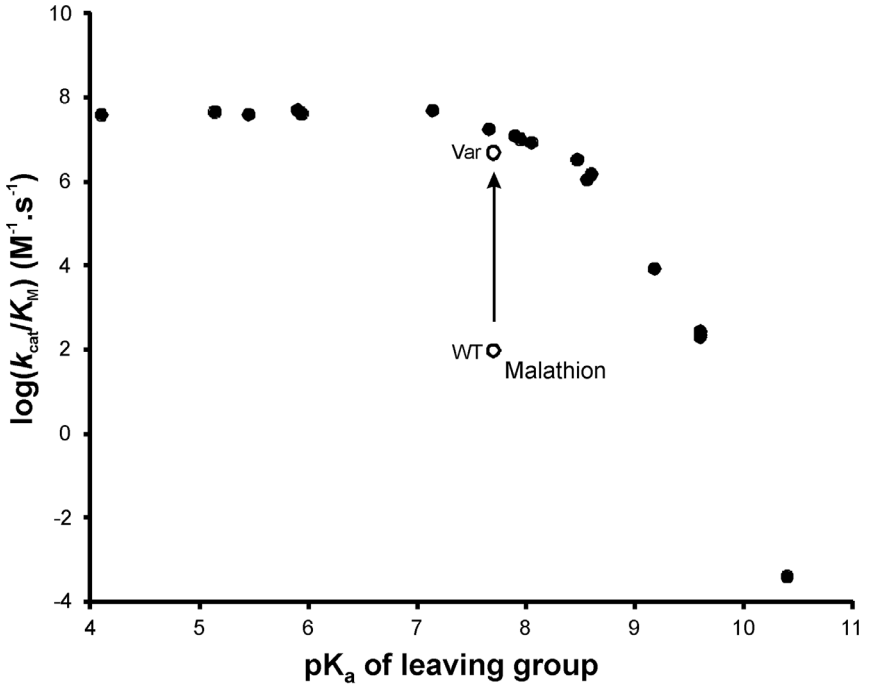

Figure 2. Brønsted plot of leaving group pKa values *vs* log(k_{cat}/K_M) for a range of substates. The pK_a values of the leaving groups 2,6-difluoro-4-nitrophenol; quinoxalin-2-ol; 2-fluoro-4-nitrophenol; 2-isopropyl-6-methylpyrimidin-4-ol; 3-fluoro-4-nitrophenol; 4-nitrophenol; 4-hydroxybenzaldehyde; 2,2-dichloroethylenol; 4-hydroxybenzonitrile; 1-(4-hydroxyphenol)ethanone; methyl 4-hydroxybenzoate; 4-hydroxybezamide; 3-chloro-7-hydroxy-4-methyl-2H-chromen-2-one; 2-(ethylthio)ethanethiol; 2-(diethylamino)ethanethiol; 2-(diisopropylamino)ethanethiol; and 4-(methoxymethyl)phenol plotted (left to right) against their log(k_{cat}/K_M) values. pK_a values were as published elsewhere [8,17,20] or as calculated using the SPARC online pK_a calculator (http://ibmlc2.chem.uga.edu/sparc/) [38]. The biphasic dependence of the enzyme on pK_a as described elsewhere [8,20] is shown: the curve flattens below a pK_a of ~8.0 and there is a linear dependence on pK_a at values below *ca*. 8.0.
doi:10.1371/journal.pone.0094177.g002

Site saturation libraries

pETMCS1-*opdA* was used as a template for the site saturation mutagenesis libraries. The method of Ho *et al.* [30] was used to make libraries of *opdA* mutants in which codons were replaced with the NNS degenerate codon. Mutant libraries targeted either single amino acid substitutions at position 106, 271 or 303 or two simultaneous amino acid substitutions at positions 60 and 61, 131 and 132, 254 and 257, 306 and 308, and 308 and 309. Each of the single substitution libraries encoded 32 variants and each of the double substitution libraries encoded 1024 variants. The library amplicons were cloned into pETMCSI [24] using *Nde*I and *Eco*RI. The diversity of mutations within each library was ascertained by sequencing plasmid DNA obtained from transformants prior to any laboratory selection.

Screening for malathion hydrolase activity

For malathion hydrolase activity screening, competent BL21 (λDE3) were transformed with libraries cloned into pETMCS1, plated on LBA and incubated at 37 °C overnight. Ninety five transformants were screened from each library with single amino acid substitutions and 3070 transformants screened from each library with double amino acid substitutions; this resulted in each library being screened at ~3× the diversity of the library. Transformants were transferred into two 96-well growth blocks (3 mL volume in each well), with each growth block containing 94 library transformants, one BL21 (λDE3) pETMCS1-*OpdA* colony (base-line control) and one BL21 (λDE3) colony (negative control).

Growth blocks were incubated at 37 °C over night then centrifuged at 5,300×g for 30 minutes to sediment the cultures. The pellets were resuspended and lysed in 3 mL Bugbuster solution (Novagen), according to the manufacturer's instructions. 40 µL of cell-free extract (CFE) from each well was transferred to a 96-well microtitre plate.

The rate of malathion hydrolysis by the CFEs was followed by measuring the rate of thiol group liberation (i.e. diethyl 2-mercaptosuccinate formation) using Ellman's reagent modified for use in 96-well microtitre plate format: 140 µl of 5 mM Ellman's reagent containing 20 mM malathion was added to 40 µl of CFE. The change in absorbance at 412 nm was measure for 30 min using a SpectraMax M2 spectrophotometer (Molecular Devices, CA).

Plasmids were obtained from transformants that possessed greater malathion hydrolase activity than the BL21 (λDE3) pETMCS1-*OpdA* control using a plasmid DNA purification kit (Macherey-Nagel, Germany), and the sequences of the *OpdA* mutants were obtained (Micromon, Melbourne).

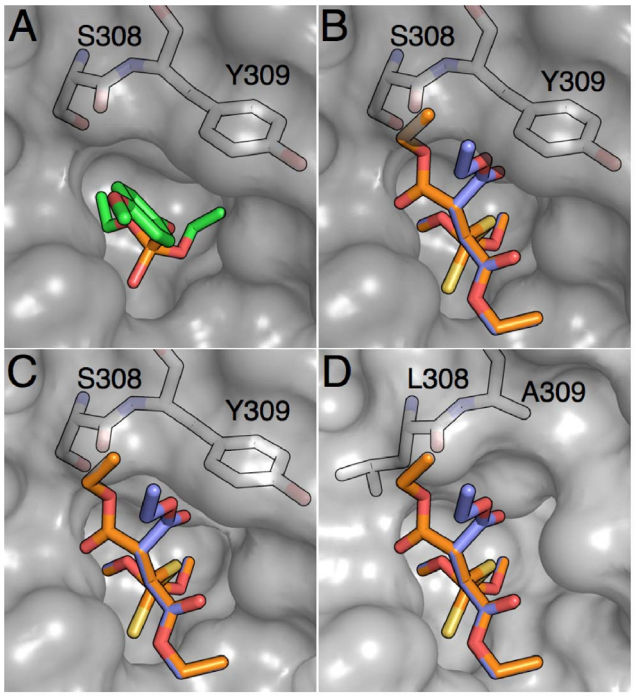

Figure 3. Docking of malathion into the crystal structures of wild-type PTE_{AR} and PTE_{AR} Ser308Leu/Tyr309Ala. A. The substrate-binding pocket of PTE_{Ar} (2R1N) with bound substrate. The amino acids that were randomised in this experiment are labelled. B. Superimposed structures of malathion docked in the active site of PTE_{Ar} in two different conformations. The branched leaving group of malathion results in steric clashes with the protein, primarily with Ser308 and Tyr309. C. Superimposed structures of malathion docked in the active site of the minor, open, conformation of PTE_{Ar} in two different conformations. The steric clash with Tyr309 is lessened. D. Superimposed structures of malathion docked in the active site of the Ser309Leu/Tyr309Ala variant of PTE_{Ar}. This shows that the Tyr309Ala mutation has opened the substrate-binding cavity, removing the steric hindrance to malathion binding in a productive conformation.
doi:10.1371/journal.pone.0094177.g003

Protein expression, purification and crystallization

PTE_{Ar} and variants were expressed in BL21 (λDE3) grown in TB supplemented with 100 µM $CoCl_2$ at 30 °C for 48 hours. The cells were harvested after 48 hours by centrifugation (5,000×g for 15 min), pellets were then resuspended in 5 ml of 50 mM HEPES with 1 mM $CoCl_2$ (pH 8) per gram of cells. Cells were lysed using an EmulsiflexC_3 homogeniser (Avestin Inc., Germany) according to the manufacturer's instructions. Cell debris was removed by centrifuging at 20,000×g for 30 minutes and the supernatant was recovered.

PTE_{Ar} and variants were purified as described elsewhere [17,19]. All columns and chromatographic media were purchased from GE Healthcare. Protein concentration was determined using a nanodrop ND-1000 spectrophotometer (Thermofisher Scientific, Australia), assuming an extinction coefficient of 29,280 $M^{-1}.cm^{-1}$ [19]. Protein purity was monitored by using reducing pre-cast SDS-PAGE gels (NuSep, Australia) stained with Coomasie brilliant blue. PTE_{Ar} was crystallised as previously described [7,18].

Crystal soaking and X-ray data collection

PTE_{Ar} crystals were serially transferred to cryoprotectant solutions consisting of 40% PEG 3350 and 0.2 M NaNO3 with or without 2 mM malathion for 2 minutes before data collection. The crystals were flash-cooled to 100 K in a cryogenic nitrogen gas stream. Diffraction data were collected on a Marresearch marµX system, comprising a Xenocs Genix^{3D} Cu high flux generator and a mar345 image plate detector. All data reduction was performed using XDS and CCP4 [31,32].

Structure determination

Crystals were isomorphous to those previously solved (space-group *P*3121, a = 108.9, c = 62.4) [7,18]; accordingly, this model was used to calculate the initial protein phases. REFMAC as implemented in the CCP4 suite of program [33], was employed for refinement. The structure and restrains for diethyl thiophosphate were taken from previous work [17]. Difference Fourier maps obtained from soaked PTE_{Ar} crystals in the absence of bound substrate/products were obtained initially, followed by inclusion of the substrates/products in the models and real-space refinement against the positive density using restraints and the COOT

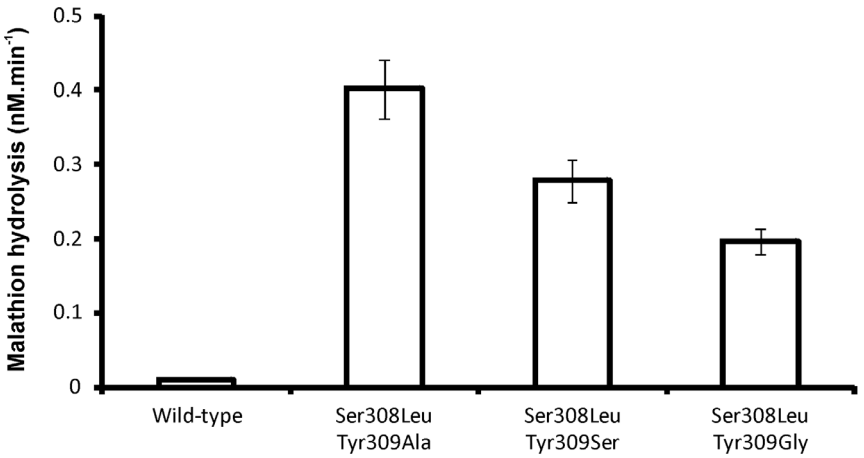

Figure 4. Screening for improved malathion hydrolase activity. The activity of three cell-free extracts from transformants isolated from the Ser308Xxx/Tyr309Xxx libraries are shown alongside that of the cell-free extract from a transformant obtained using the unmodified gene. The library transformants were subsequently shown to carry the Ser308Leu substitution and an Ala, Ser or Gly at 309. The data presented here are the averages of three independent assays, replicates varied by less than 10%.
doi:10.1371/journal.pone.0094177.g004

program [34]. These were further refined using REFMAC. Ligand occupancy was adjusted until the B-factors of the ligands refined to values comparable to the interacting metal ions/amino acids.

Enzyme assays

Rates of hydrolysis of malathion and demeton were measured by quantifying the formation of thiol groups using the modified Ellman's assay [35], essentially as described above, 140 µl of 5 mM Ellman's reagent containing malathion or demeton (0, 5, 10, 25, 50, 100, 150, 300, 400 and 600 µM) was added to 40 µl of 50 mM HEPES buffer containing 0.22–0.43 nM enzyme, as appropriate. Each assay was conducted in triplicate. An extinction co-efficient of 14,140 $M^{-1}.cm^{-1}$ [35] was used. Hydrolysis rates for diazinon, chlorpyrifos and parathion were obtained spectrophotometrically, as described elsewhere [10]. Rates were determined over 30 minutes. Values for k_{cat} and K_M were estimated using "Hyper32" hyperbolic regression software [20].

Computational procedures

Docking of malathion to the PTE_{Ar} native structure with a water molecule bridging the metal centres was performed using CDOCKER as implemented in Accelrys Discovery Studio [36]. The top 10 poses were taken from a run docking 40 orientations of 40 conformers of malathion with simulated annealing for each pose.

Results and Discussion

Malathion is a poor substrate for PTE_{Ar}

PTE_{Ar} has a k_{cat}/K_M value for malathion of 4×10^2 $s^{-1}.M^{-1}$. The pK_a of the leaving group of malathion (diethyl 2-mercaptosuccinate) is predicted to be 7.7, suggesting that malathion is turned over by PTE_{Ar} with a k_{cat}/K_M that is at least several order of magnitude lower than other phosphotriesters with leaving groups that have similar pK_a values (Fig. 2). This suggests that another parameter, such as substrate binding or formation of the Michaelis complex, may limit the rate of this reaction.

Table 1. Kinetic parameters of purified PTE_{Ar} and most active variant against malathion for a range of OP insecticides.

Substrate		Wild Type		PTE_{Ar}	Ser308Leu	/Tyr309Ala
	$k_{cat}(s^{-1})$	$K_M(\mu M)$	$k_{cat}/K_M(s^{-1}.M^{-1})$	$k_{cat}(s^{-1})$	$K_M(\mu M)$	$k_{cat}/K_M(s^{-1}.M^{-1})$
Malathion	3.9×10^{-2}	1100	3.5×10^{1}	7.6×10^{2}	410	1.9×10^{6}
	(2.1×10^{-3})	(97)		(3.3×10^{1})	(35)	
Parathion	6.2×10^{3}	330	1.9×10^{7}	9.1×10^{2}	340	2.7×10^{6}
	(9.3×10^{1})	(25)		(8.2×10^{1})	(31)	
Demeton	1.4×10^{-2}	490	2.9×10^{1}	1.1×10^{-2}	490	2.2×10^{1}
	(1.4×10^{-3})	(39)		(9.3×10^{-4})	(17)	
Diazinon	1.0×10^{3}	480	2.1×10^{6}	1.1×10^{3}	430	2.5×10^{7}
	(9.6×10^{1})	(46)		(8.4×10^{1})	(39)	
Chlorpyrifos	3.8×10^{1}	290	4.3×10^{5}	2.3×10^{1}	220	1.0×10^{6}
	(2.6×10^{0})	(27)		(2.1×10^{0})	(13)	

Standard deviations for the k_{cat} and K_M values are given in parentheses below the mean values obtained for triplicate experiments.
doi:10.1371/journal.pone.0094177.t001

Table 2. Data collection and refinement statistics for structures reported in this work.

	PTE_{Ar} Ser308Leu/Tyr309Ala	PTE_{Ar}+2 mM malathion Ser308Leu/Tyr309Ala
Space group	P3 12 1	P3 12 1
Unit-cell parameters		
a (Å)	57.09	109.10
b (Å)	101.80	109.10
c (Å)	79.89	63.43
α,β,γ (°)	90, 90, 120	90, 90, 120
Data collection		
Wavelength (Å)	1.5418	1.5418
Resolution range (Å)*	29.36–1.99 (2.04–1.99)	28.22–1.99 (2.04–1.99)
No. of unique reflections	29386	30260
Redundancy	10.8 (9.9)	7.2 (6.6)
Completeness (%)	99.8 (97.8)	99.8 (98.4)
$R_{merge(I)}$ †	0.122 (0.750)	0.123 (0.889)
Mean $<I/\sigma(I)>$	20.2 (4.0)	15.4 (2.4)
$CC_{1/2}$ ‡	(0.998) (0.877)	0.997 (0.734)
Refinement		
No. reflections (total)	27872	28317
Resolution range	29.36–1.99 (2.04–1.99)	28.22–1.99(2.04–1.99)
R_{work}/R_{free} ‡	0.158/0.186 (0.212/0.278)	0.206/0.251 (0.266–0.319)
R.m.s deviations		
Bond lengths (Å)	0.022	0.019
Bond angles (°)	2.084	2.036
PDB ID	3WML	4NP7

*Values in parenthesis are for the highest-resolution shell.
†$R_{merge(I)} = (\Sigma_{hkl}\ \Sigma_j\ |I_{hkl,j}-\langle I_{hkl}\rangle|)/(\Sigma_{hkl}\ \Sigma_j\ I_{hkl,j})$ where $\langle I_{hkl}\rangle$ is the average intensity of *j* symmetry-related observations of reflections with Miller indices *hkl*.
‡$CC_{1/2}$ = percentage of correlation between intensities from random half-datasets.
‡$R_{work} = \Sigma_{hkl}|F_{(obs)}-F_{(calc)}|/\Sigma_{hkl}|F_{(obs)}|$; 5% of the data that were excluded from the refinement were used to calculate R_{free}.
doi:10.1371/journal.pone.0094177.t002

To rationalise the very low kinetic parameters of PTE_{Ar} with malathion, we performed a series of computational docking procedures using the CDOCKER algorithm. CDOCKER has previously been verified crystallographically with PTE_{Ar}, producing a docked pose that was essentially superimposable with a crystal structure of an PTE_{Ar}-diethyl 4-methoxyphenyl phosphate complex [17](Fig. 3A). Forty orientations of forty conformers of malathion were docked, with simulated annealing for each pose. The results did not yield any poses that were productively bound with the substrate appropriately aligned for nucleophilic attack from the metal-ion coordinated nucleophile. To investigate further, we superimposed various conformers of malathion onto the substrate in a crystallographic PTE_{Ar}:substrate complex (Fig. 3). This revealed that the substrate binding pocket was too small to accommodate the branched leaving group of malathion, with particular clashes near Ser308 and Tyr309 (Fig. 3B).

If malathion cannot bind to PTE_{Ar}, then how can the low, but significant, turnover of this substrate be explained? Previous work was shown that PTE_{Ar} fluctuates between open and closed conformations [37], and that alternative open conformations allowed the binding of another larger organophosphate, chlorfenvinfos [20]. When malathion is docked into this minor, open, conformation, it is clear that the steric clashes no longer prevent binding, i.e. a minor conformation appears to catalyze a non-native activity (Fig. 3C). This low-level promiscuous activity towards malathion, coupled with the relatively good leaving group of this substrate, suggests that significant increases in activity should be possible, provided the substrate binding site is sufficiently modified to favour formation of the Michaelis complex.

CASTing for improved malathion hydrolysis

In accordance with the docking results, a semi-rational approach was used to improve the turnover of this substrate. CASTing was performed in the substrate-binding pocket of PTE_{Ar}, with each of the residues that form the substrate-binding pocket included in at least one CASTing library. CASTing is an approach wherein analysis of an enzyme's 3D structure is used to identify groups of two or three amino acids from the binding-pocket, which are then randomized simultaneously to create relatively small libraries of mutants that can be screened with relatice ease. For PTE_{Ar}, each CASTing library carried substitutions at one or two amino acid positions and therefore producing libraries of 32 or 1024 variants (using an NNS degeneracy). The libraries were: Gly60Xxx and Ser61Xxx, Ile106Xxx, Trp131Xxx and Phe132Xxx, Arg254Xxx and Tyr257Xxx, Leu271Xxx, Leu303Xxx, Phe306Xxx and Ser308Xxx, and Ser308Xxx and Tyr309Xxx. Cell-free extract from each library was screened for the rate of formation of free thiol (as a result of malathion hydrolysis; Fig. 1), with 95 or 3070 transformants screened per library depending upon the size of the library screened (i.e, screened at $\sim 3\times$ the diversity of the library).

Although the majority of transformants from all libraries retained some hydrolytic activity against malathion, only the library in which Ser308 and Tyr309 were targeted for mutagenesis provided variants with increased activity towards malathion compared with that of the wild-type enzyme (Fig 4). Variants with increased rates of malathion activity were found to carry a Ser308Leu substitution and a substitution of Tyr309 for Gly, Ser or Ala. Site-directed mutants of wild-type *opdA* were constructed that encoded only substitutions of Tyr309 for Gly, Ser or Ala; however, the expressed variants were insoluble.

The steady-state kinetic parameters of the most active variant (Ser308Leu, Tyr309Ala) were obtained and compared with those of the wild-type enzyme. There was a 2.7-fold decrease in the K_M for malathion (410 *vs.* 1,100 μM; Table 1) and a 2×10^4-fold increase in k_{cat}, (7.7×10^2 *vs.* 3.9×10^{-2} s^{-1}; Table 1), leading to a 5.4×10^4-fold increase in the k_{cat}/K_M (1.9×10^5 *vs.* 3.5×10^1 $s^{-1}.M^{-1}$; Table 1). Thus, amino acid substitutions at positions 308 and 309 alleviate the majority of the limitation on the rate of malathion hydrolysis by PTE_{Ar}. Such large changes in turnover rates were not observed with a range of other OP insecticides including parathion (ca. 5-fold reduction in k_{cat}/K_M value), *ca.* 2- and 9-fold increases in k_{cat}/K_M values for chlorpyrifos and diazinon respectively, and no significant change in the rate of demeton turnover (Table 1). These data suggest that the specific interaction between PTE_{Ar} and malathion *via* amino acids at positions 308 and 309 was responsible for the low turnover of malathion by the wild-type enzyme.

Crystallographic analysis of PTE_{Ar} Ser308Leu/Tyr309Ala

In order to rationalise the effects of these mutations, we solved the crystal structure of the PTE_{Ar} Ser308Leu/Tyr309Ala mutant (crystallographic data in Table 2). This did not reveal any significant changes to the backbone or B-factors of the loop that these mutations are located on (Loop 7). However, the Tyr309Ala mutation did expand the size of the active site entrance substantially (Fig. 3D). To investigate whether the enzyme, as constrained by the crystal packing, could still hydrolyze malathion, we performed a crystal soaking experiment, in which we soaked the crystal in 1 mM malathion for two minutes. The structural model obtained from the soaked crystal revealed density in the active site matching the product diethyl thiophosphate, in a known product binding mode [17]. This establishes that the crystal structure observed here is capable of hydrolysing malathion at rapid rates.

To investigate whether this increase in activity was a result of relieving the steric hindrance that was inhibiting substrate turnover in the wild-type enzyme, we performed substrate docking with malathion and the engineered Ser308Leu/Tyr309Ala variant (Fig. 3D). These results confirmed that the widening of the active site that occurs as a result of these mutations allows productive substrate binding and vastly improved turnover rates. It also explains the reduced turnover of paraoxon (Table 1): previous work has established that the interaction between the aromatic group of Tyr309 and the aromatic group of paraoxon, which is lost in this mutant, enhances catalysis.

Summary

PTE_{Ar} has potential in a wide range of applications, due its high turnover rates and broad substrate specificity. However, the applicability of the wild-type enzyme is limited for some substrates, such as malathion. Here we have enhanced the turnover rate for malathion by ~5,000 fold using a semi-rational approach, which has alleviated the steric hindrance responsible for the low rate of malathion turn-over in the wild-type enzyme. The requirement for two amino acid substitutions, adjacent to each other in the protein, suggests that it would have been unlikely to have produced this specific variant by another, purely random, method.

Author Contributions

Conceived and designed the experiments: TN ACW ES PDC CJJ CS. Performed the experiments: TN ACW NF ES PDC. Analyzed the data: TN ACW ES PDC CJJ CS. Wrote the paper: TN ACW CJJ CS.

References

1. Eddleston M, Buckley NA, Eyer P, Dawson AH (2008) Management of acute organophosphorus pesticide poisoning. Lancet 371: 597–607.
2. Paudyal BP (2008) Organophosphorus Poisoning. Journal of Nepal Medical Association 47: 251–258.
3. Russell RJ, Scott C, Jackson CJ, Pandey R, Pandey G, et al. (2011) The evolution of new enzyme function: lessons from xenobiotic metabolizing bacteria versus insecticide-resistant insects. Evolutionary Applications 4: 225–248.
4. Jackson CJ, Liu JW, Carr PD, Younus F, Coppin C, et al. (2011) Structure and function of an insect alpha-carboxylesterase (alpha Esterase7) associated with insecticide resistance. Proceedings of the National Academy of Sciences of the United States of America 110: 10177–10182.
5. Dumas DP, Caldwell SR, Wild JR, Raushel FM (1989) Purification and properties of the phosphotriesterase from *Pseudomonas diminuta*. Journal of Biological Chemistry 264: 19659–19665.
6. Horne I, Sutherland TD, Harcourt RL, Russell RJ, Oakeshott JG (2002) Identification of an *opd* (organophosphate degradation) gene in an *Agrobacterium* isolate. Applied and Environmental Microbiology 68: 3371–3376.
7. Jackson CJ, Carr PD, Kim HK, Liu JW, Herrald P, et al. (2006) Anomalous scattering analysis of Agrobacterium radiobacter phosphotriesterase: the prominent role of iron in the heterobinuclear active site. Biochemical Journal 397: 501–508.
8. Caldwell SR, Newcomb JR, Schlecht KA, Raushel FM (1991) Limits of diffusion in the hydrolysis of substrates by the phosphotriesterase from *Pseudomonas dimunuta*. Biochemistry 30: 7438–7444.
9. Wille T, Scott C, Thiermann H, Worek F (2012) Detoxification of G- and V-series nerve agents by the phosphotriesterase OpdA. Biocatalysis and Biotransformation 30.
10. Scott C, Begley C, Taylor MJ, Pandey G, Momiroski V, et al. Free-Enzyme Bioremediation of Pesticides: A case study for the enzymatic remediation of organophosphorous insecticide residues. In: Goh KS, Gan J, Bret B, editors. ACS Symposium Series; 2011; CA. American Chemical Society.
11. Jackson CJ, Scott C, Carville A, Mansfield K, Ollis DL, et al. (2010) Pharmacokinetics of OpdA, an organophosphorus hydrolase, in the African green monkey. Biochemical Pharmacology 80: 1079–1086.
12. Weston DP, Jackson CJ (2009) Use of Engineered Enzymes to Identify Organophosphate and Pyrethroid-Related Toxicity in Toxicity Identification Evaluations. Environmental Science & Technology 43: 5514–5520.
13. Bird SB, Sutherland TD, Gresham C, Oakeshott J, Scott C, et al. (2008) OpdA, a bacterial organophosphorus hydrolase, prevents lethality in rats after poisoning with highly toxic organophosphorus pesticides. Toxicology 247: 88–92.
14. Dawson RM, Pantelidis S, Rose HR, Kotsonis SE (2008) Degradation of nerve agents by an organophosphate-degrading agent (OpdA). Journal of Hazardous Materials 157: 308–314.
15. Scott C, Pandey G, Hartley CJ, Jackson CJ, Cheesman MJ, et al. (2008) The enzymatic basis for pesticide bioremediation. Indian Journal of Microbiology 48: 65–79.
16. Aubert SD, Li YC, Raushel FM (2004) Mechanism for the hydrolysis of organophosphates by the bacterial phosphotriesterase. Biochemistry 43: 5707–5715.
17. Jackson CJ, Foo JL, Kim HK, Carr PD, Liu JW, et al. (2008) *In crystallo* capture of a Michaelis complex and product-binding modes of a bacterial phosphotriesterase. Journal of Molecular Biology 375: 1189–1196.
18. Jackson C, Kim HK, Carr PD, Liu JW, Ollis DL (2005) The structure of an enzyme-product complex reveals the critical role of a terminal hydroxide nucleophile in the bacterial phosphotriesterase mechanism. Biochimica Et Biophysica Acta-Proteins and Proteomics 1752: 56–64.
19. Jackson CJ, Liu JW, Coote ML, Ollis DL (2005) The effects of substrate orientation on the mechanism of a phosphotriesterase. Organic & Biomolecular Chemistry 3: 4343–4350.
20. Jackson CJ, Weir K, Herlt A, Khurana J, Sutherland TD, et al. (2009) Structure-based rational design of a phosphotriesterase. Applied and Environmental Microbiology 75: 5153–5156.

21. Cho CM, Mulchandani A, Chen W (2002) Bacterial cell surface display of organophosphorus hydrolase for selective screening of improved hydrolysis of organophosphate nerve agents. Appl Environ Microbiol 68: 2026–2030.
22. Watkins LM, Mahoney HJ, McCulloch JK, Raushel FM (1997) Augmented hydrolysis of diisopropyl fluorophosphate in engineered mutants of phosphotriesterase. Journal of Biological Chemistry 272: 25596–25601.
23. Cho CMH, Mulchandani A, Chen W (2004) Altering the substrate specificity of organophosphorus hydrolase for enhanced hydrolysis of chlorpyrifos. Applied and Environmental Microbiology 70: 4681–4685.
24. Yang H, Carr PD, McLoughlin SY, Liu JW, Horne I, et al. (2003) Evolution of an organophosphate-degrading enzyme: a comparison of natural and directed evolution. Protein Eng 16: 135–145.
25. Bonner MR, Coble J, Blair A, Freeman LEB, Hoppin JA, et al. (2007) Malathion exposure and the incidence of cancer in the agricultural health study. American Journal of Epidemiology 166: 1023–1034.
26. Schleier JJ, Peterson RKD, Irvine KM, Marshall LM, Weaver DK, et al. (2012) Environmental fate model for ultra-low-volume insecticide applications used for adult mosquito management. Science of the Total Environment 438: 72–79.
27. Edwards JW, Lee SG, Heath LM, Pisaniello DL (2007) Worker exposure and a risk assessment of Malathion and Fenthion used in the control of Mediterranean fruit fly in South Australia. Environmental Research 103: 38–45.
28. Reetz MT, Wang LW, Bocola M (2006) Directed evolution of enantioselective enzymes: Iterative cycles of CASTing for probing protein-sequence space. Angewandte Chemie-International Edition 45: 1236–1241.
29. Tartoff KD, Hobbs CA (1987) Improved Media for Growing Plasmid and Cosmid Clones. Bethesda Research Laboratory Focus: 12.
30. Ho SN, Hunt HD, Horton RM, Pullen JK, Pease LR (1989) Site-directed mutagenesis by overlap extension using the polymerase chain-reaction. Gene 77: 51–59.
31. Kabsch W (2010) XDS. Acta Crystallographica Section D-Biological Crystallography 66: 125–132.
32. Bailey S (1994) The CCP4 suite – programs for protein crystallography. Acta Crystallographica Section D-Biological Crystallography 50: 760–763.
33. Murshudov GN, Skubak P, Lebedev AA, Pannu NS, Steiner RA, et al. (2011) REFMAC5 for the refinement of macromolecular crystal structures. Acta Crystallographica Section D-Biological Crystallography 67: 355–367.
34. Emsley P, Lohkamp B, Scott WG, Cowtan K (2010) Features and development of Coot. Acta Crystallographica Section D-Biological Crystallography 66: 486–501.
35. Ellman GL, Courtney KD, Andres V, Featherstone RM (1961) A new and rapid colorimetric determination of acetylcholinesterase activity. Biochemical Pharmacology 7: 88–&.
36. Accelrys Discovery Studio (2012) San Diego: Accelrys Software Inc. Accelrys Discovery Studio modeling environment, release 3.5.
37. Jackson CJ, Foo JL, Tokuriki N, Afriat L, Carr PD, et al. (2009) Conformational sampling, catalysis, and evolution of the bacterial phosphotriesterase. Proceedings of the National Academy of Sciences of the United States of America 106: 21631–21636.
38. Hilal S, Karickhoff SW, Carreira LA (1995) A rigorous test for SPARC's chemical reactivity models: estimation of more than 4300 ionization pKa's. Quantitative Structure-Activity Relationships 14:348–355.